Molecular Tectonics of Entangled Metal-Organic Frameworks Based on Different Conformational Carboxylates Mixed with a Flexible N,N '-Type Ligand

ARTICLE *in* CRYSTAL GROWTH & DESIGN · FEBRUARY 2011

Impact Factor: 4.89 · DOI: 10.1021/cg101461w

4 AUTHORS, INCLUDING:

Jianqiang Liu
Guangdong Medical College
65 PUBLICATIONS **920** CITATIONS

SEE PROFILE

Ying-Yong Zhao
Northwest University
103 PUBLICATIONS **1,144** CITATIONS

SEE PROFILE

DOI: 10.1021/cg101461w

CRYSTAL GROWTH & DESIGN Article

2011, Vol. 11
569–574

Molecular Tectonics of Entangled Metal−Organic Frameworks Based on Different Conformational Carboxylates Mixed with a Flexible N,N′-Type Ligand

Jian-Qiang Liu,*,† Yun-Sheng Huang,† Ying-Yong Zhao,‡ and Zhen-Bin Jia†

†*Guangdong Medical College, School of Pharmacy, Dongguan, 523808, P. R. China, and* ‡*Biomedicine Key Laboratory of Shaanxi Province, the College of Life Sciences, Northwest University, No. 229 Taibai North Road, Xi'an, Shaanxi 710069, China*

Received November 4, 2010; Revised Manuscript Received December 7, 2010

ABSTRACT: On the basis of 1,4-bis(2-methyl-imidazol-1-yl)butane (bib), three new coordination polymers, namely, $[Co(L1)(bib)]_n$ (**1**), $\{[Co(L2)(bib)]\cdot 1.5H_2O\}_n$ (**2**), and $\{[Co(L3)(bib)_{0.5}]\cdot H_2O\}_n$ (**3**) (H_2L1 = *m*-phthalic acid, H_2L2 = glutaric acid, and H_2L3 = 1,4-phenylenediacetic acid), have been synthesized and characterized. Polymer **1** features a three-dimensional (3D) 3-fold interpenetrating $CdSO_4$ motif containing multiple interweaving helical chains. Compound **2** displays a 3D 3-fold interpenetrating 3-connected **ThSi$_2$** architecture with intriguing *pseudo*-Borromean links. Complex **3** shows a 3D 2-fold interpenetrating **Pcu** net. The results reveal that the dicarboxyl building blocks with different conformations play a significant role in promoting the diversity of the observed structural motifs. In addition, the magnetic property of **3** is also studied.

Introduction

Recently, various kinds of metal−organic frameworks (MOFs) with fascinating topological motifs and desirable properties have been identified and documented.[1−3] The interpenetration, as the most investigated type of entanglement, has been discussed in comprehensive reviews by Robson, Batten, Ciani, Champness.[4] More merits of the interpenetrating networks have been discovered.[5] Some researchers proved interpenetration would be utilized to strengthen the interaction between the gaseous molecule and the net by an entrapment mechanism.[6] However, the crystallization is a very complicated process. The formation of molecular motifs depends on the combination of several factors, such as the coordination geometry of central metal and the nature of the organic ligand.[7] In this regard, the selection of organic ligands with appropriate backbones would be a critical step in modulating the resultant topologies of metal−organic frameworks. The employment of mixed ligands during the self-assembly process has gradually become an effective approach, which is expected to obtain nets showing more diverse structural topologies.[8] So far, more carboxylate linkers are widely utilized in the construction of MOFs.[9] However, MOFs containing carboxylates and flexible N-bridging ligands, especially bis(imidazole) ligands, are relatively rare.[10]

Generally, longer ligands will give rise to larger voids. It can be said that the larger voids in the 3D motif, the more likely interpenetration will be observed.[11] The flexible ligand of 1,4-bis(2-methyl-imidazol-1-yl)butane (bib), which is synthesized according to the literature,[10i] is our choice for construction entangled MOFs (Scheme 1). Bib with a $-CH_2-CH_2-CH_2-CH_2-$ spacer is a good candidate for N-donor linker. The flexible nature of the $-(CH_2)_4-$ spacer allows the molecule to bend and rotate freely when binding to metal centers so as to conform to the coordinative geometries of metal ions. Up to now, some MOFs with flexible bis(imidazole) ligands (e.g., 1,1′-(1,4-butanediyl)bis(imidazole) and 1,1′-(1,6-hexanedily)bis(imidazole)) have been investigated.[10] A variety of entangled polymers with 1,1′-(1,4-butanediyl)bis(imidazole) (bim) have been prepared, including self-interpenetration, "real" interpenetration, and polycatenation (Table S1, Supporting Information). Recently, we have focused on a flexible bis(imidazole) ligand, 1,4-bis(2-methyl-imidazol-1-yl)butane (bib), as a powerful precursor, which controls the dimensionality of the final product.[12] Compared to 1,1′-(1,4-butanediyl)-bis(imidazole), the presence of a pair of methyl groups of bib may be beneficial for tuning the size and surface property of the pores. It has been observed that steric hindrance could be taken as tool for maneuvering the topologies and interpenetrating dimensions.[1a,8c] Therefore, a pair of methyl groups can be expected to create enough steric hindrance to restrict the metal center from adopting a higher coordination number. On the other hand, angular and flexible disposition of the coordination atoms of the auxiliary ligand plays an important role in modulating the network topologies.[8c] The employment of aromatic/aliphatic polycarboxylic acids would impose kinds of angular dispositions of coordination atoms (Scheme 1). In the present contribution, we report three new three-dimensional (3D) MOFs, $[Co(L1)(bib)]_n$ (**1**), $\{[Co(L2)(bib)]\cdot 1.5H_2O\}_n$ (**2**), and $\{[Co(L3)(bib)_{0.5}]\cdot H_2O\}_n$ (**3**) (H_2L1 = *m*-phthalic acid; H_2L2 = glutaric acid, and H_2L3 = 1,4-phenylenediacetic acid), constructed from cobalt salts and bib in the presence of carboxylates with different conformations. All of them exhibit intriguing interpenetrating frameworks with distinct topologies.

Experimental Section

Materials and Instruments. All reagents were purchased from commercial sources and used as received; the bib was synthesized according to the literature.[10i] IR spectra were recorded with a Perkin−Elmer Spectrum One spectrometer in the region 4000−400 cm^{-1} using KBr pellets. Thermogravimetric analyses (TGA) were carried out with a Metter−Toledo TA 50 in dry nitrogen atmosphere (60 mL min^{-1}) at a heating rate of 5 °C min^{-1}.

*To whom correspondence should be addressed.

Published on Web 12/31/2010

X-ray power diffraction (XRPD) data were recorded on a Rigaku RU200 diffractometer at 60 kV, 300 mA for Cu K_α radiation (λ = 1.5406 Å), with a scan speed of 2 °C/min and a step size of 0.02° in 2θ. Magnetic susceptibility data of powdered sample restrained in parafilm were measured on Oxford Maglab 2000 magnetic measurement system in the temperature range 300−2 K and at field of 1 kOe.

X-ray Crystallography. Single crystal X-ray diffraction analyses of the three compounds were carried out on a Bruker SMART APEX II CCD diffractometer equipped with a graphite monochromated MoKα radiation (λ = 0.71073 Å) by using ϕ/ω scan technique at room temperature. The intensities were corrected for Lorentz and polarization effects as well as for empirical absorption based on multiscan techniques; all structures were solved by direct methods and refined by full-matrix least-squares fitting on F^2 by SHELX-97.[13] Absorption corrections were applied by using multiscan program SADABS.[14] The hydrogen atoms of organic ligands were placed in calculated positions and refined using a riding on attached atoms with isotropic thermal parameters 1.2 times those of their carrier atoms. The water hydrogen atoms were located from difference maps and refined with isotropic thermal parameters 1.5 times those of their carrier atoms. The hydrogen atoms of one lattice water molecule (O5) in compound **2** were not located using the different Fourier method. The hydrogen atoms on the solvent water molecule were included in the total atomic formula, but they are not included in the list of atoms. Table 1 shows crystallographic data of **1**−**3**. Selected bond distances and bond angles and parameters are listed in Table 2 (CCDC: 780291−780293).

Synthesis of These Complexes. [Co(L1)(bib)]$_n$ (1). A mixture of **$CoSO_4 \cdot 7H_2O$** (0.029 g, 0.1 mmol), H_2L1 (0.017 g, 0.1 mmol), bib (0.022 mg, 0.1 mmol), NaOH (0.05 mmol), CH_3OH (2 mL), and deionized water (8 mL) was stirred for 30 min in air, then transferred and sealed in a 25-mL Teflon reactor, which was heated at 150 °C for 72 h. The solution was then cooled to room temperature at a rate of 5 °C h^{-1}, to yield a very fine pink crystalline product **1** in 50% yield based on Co. $C_{20}H_{22}CoN_4O_4$ (441.35) Calcd: C, 54.23; H, 5.02; N, 12.69. Found C, 54.30; H, 4.89; N, 12.58. IR (KBr, cm^{-1}): 3028(w), 2818(w), 1580(s), 1418(s), 1080(m), 612(m).

{[Co(L2)(bib)]·1.5H_2O}$_n$ (2). The synthesis procedure of **2** was similar to that of **1** except that H_2L1 was replaced by H_2L2 (0.1 mmol). $C_{34}H_{54}Co_2N_8O_{11}$ (868.71). C, 47.01; H, 6.27; N, 12.90. Found C, 46.95; H, 6.19; N, 12.88. IR (KBr, cm^{-1}): 3421(s), 2910(w), 1590(s), 1468(s), 1100 (w), 655(m).

Scheme 1. Diagram of Ligands in This Work

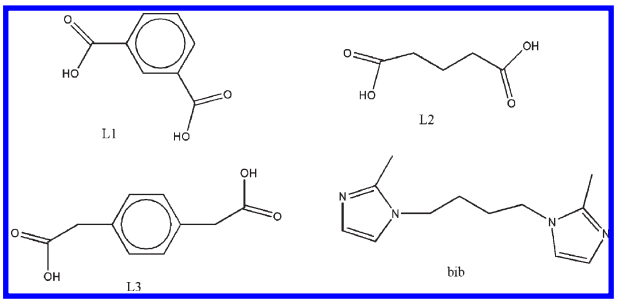

Table 2. Selected Bond Distances (Å) and Angles (°)

Complex **1**[a]			
O(4)−Co(1)#1	1.967(3)	N(4)−Co(1)#2	2.036(3)
Co(1)−N(4)#4	2.036(3)	Co(1)−N(1)	2.044(3)
O(4)#3−Co(1)−O(1)	130.99(11)	O(4)#3−Co(1)−N(4)#4	95.28(12)
O(1)−Co(1)−N(4)#4	115.31(13)	O(4)#3−Co(1)−N(1)	118.52(13)
O(1)−Co(1)−N(1)	95.11(12)	N(4)#4−Co(1)−N(1)	98.10(14)
Complex **2**[b]			
O(3)−Co(1)#1	2.0291(16)	N(4)−Co(1)#2	2.0182(18)
Co(1)−O(1)	1.9540(16)	Co(1)−N(1)	2.0461(17)
O(1)−Co(1)−N(4)#2	119.37(7)	O(1)−Co(1)−O(3)#3	103.59(7)
N(4)#2−Co(1)−O(3)#3	121.12(7)	O(1)−Co(1)−N(1)	114.01(8)
N(4)#2−Co(1)−N(1)	98.70(7)	O(3)#3−Co(1)−N(1)	98.23(7)
Complex **3**[c]			
O(4)−Co(1)#1	2.0735(13)	Co(1)−O(3)	2.0307(13)
Co(1)−O(1)	2.0337(14)	Co(1)−O(2)#1	2.0371(14)
Co(1)−N(1)	2.0418(15)		
O(2)#2−Co(1)−N(1)	96.87(6)	O(3)−Co(1)−O(4)#1	161.75(6)
O(1)−Co(1)−O(4)#1	88.84(6)	O(2)#2−Co(1)−O(4)#1	86.37(6)
N(1)−Co(1)−O(4)#1	93.04(6)	O(3)−Co(1)−Co(1)#1	87.07(4)
O(1)−Co(1)−Co(1)#1	84.81(4)	N(1)−Co(1)−Co(1)#1	166.38(4)

[a] Symmetry codes: #1 $-x-1, -y, z+1/2$; #2 $-x+1/2, y+1/2, z-1/2$; #3 $-x-1, -y, z-1/2$; #4 $-x+1/2, y-1/2, z+1/2$. [b] Symmetry codes: #1 $x+1/4, -y+1/4, z-3/4$; #2 $-x+1, -y, z$; 3 $x-1/4, -y+1/4, z+3/4$. [c] Symmetry codes: $-x+1, -y+1, -z+1$.

Table 1. Crystal Data and Structure Refinement Information for Compounds 1−3

compounds	1	2	3
formula	$C_{20}H_{22}CoN_4O_4$	$C_{34}H_{54}Co_2N_8O_{11}$	$C_{16}H_{19}CoN_2O_5$
fw	441.35	868.71	378.26
temp (K)	298(2)	298(2)	298(2)
cryst system	orthorhombic	orthorhombic	triclinic
space group	*Pna*21	*Fdd*2	$P\bar{1}$
a (Å)	9.3917(11)	17.721(3)	8.4306(4)
b (Å)	14.1197(16)	52.356(8)	10.8660(5)
c (Å)	15.3130(17)	8.5857(12)	10.9357(5)
α (°)	90	90	100.6540(10)
β (°)	90	90	103.8780(10)
γ (°)	90	90	111.9100(10)
V (Å^3)	2030.6(4)	7966(2)	859.41(7)
Z	4	8	2
F(000)	916	3648	392
D_c (g/cm^3)	1.444	1.449	1.462
GOF	0.860	1.054	1.091
reflections collected	3524	3397	3030
unique reflections	9611 (R_{int} = 0.0288)	9667(R_{int} = 0.0263)	7004(R_{int} = 0.0390)
final *R* indices	R_1 = 0.0375	R_1 = 0.0240	R_1 = 0.0264
(R^a ($I > 2\sigma(I)$))	wR_2 = 0.0990	wR_2 = 0.0595	wR_2 = 0.0793
R indices	R_1 = 0.0442	R_1 = 0.0260	R_1 = 0.0290
(all data)	wR_2 = 0.1060	wR_2 = 0.0607	wR_2 = 0.0803

[a] $R_1 = \sum||F_0| - |F_c||/\sum|F_0|$, $wR_2 = \{\sum[w(F_0^2 - F_c^2)^2]/\sum(F_0^2)^2\}^{1/2}$.

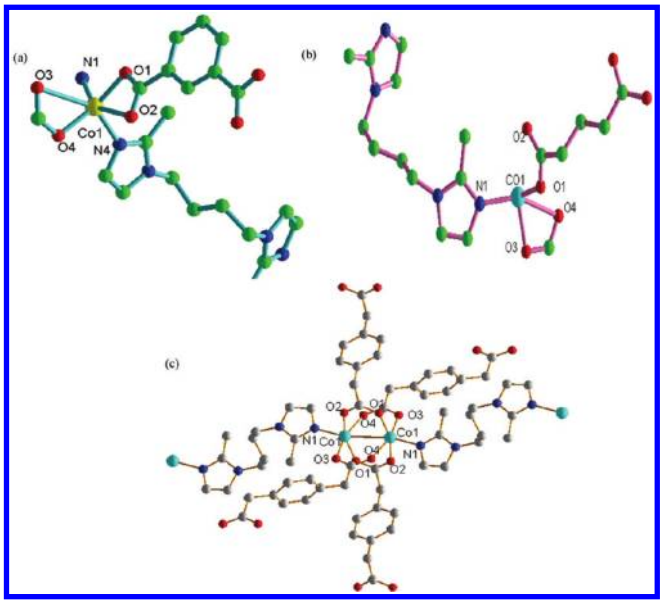

Figure 1. (a) The coordination geometry of the Co(II) center and the ligand geometry for compound **1**; (b) coordination environment of the Co(II) for compound **2**; (c) coordination environment of the Co(II) for compound **3**.

{[Co(L3)(bib)$_{0.5}$]·H$_2$O}$_n$ (3). The synthesis procedure of **3** was similar to that of **1** except that H_2L1 was replaced by H_2L3 (0.1 mmol). $C_{16}H_{19}CoN_2O_5$ (378.26). C, 50.80; H, 5.06; N, 7.41. Found C, 50.77; H, 5.01; N, 7.50. IR (KBr, cm^{-1}): 3506(s), 2899(w), 1458(vs), 981 (w), 703(m).

Results and Discussion

[Co(L1)(bib)]$_n$ (1). The asymmetry unit contains one independent cobalt atom, one L1, and one bib ligand. The Co(II) is coordinated by two oxygen atoms from two adjacent L1 ligands and two nitrogen atoms from bib linkers to give the CoO2N2 tetrahedral geometry (Figure 1a). The Co−O/N bond lengths are in the range of 1.967(3)−2.044(3) Å, which are comparable to those reported in other relative Co(II) polymers.[15] The completely deprotonated L1 ligand shows a bi(monodentate) coordinated manner, while the bib adopts a *syn-anti* coordinated fashion.

The Co(II) cations are bridged by L1 to form a 1D zigzag chain, as shown in Figure 2a. These chains are further connected by bridging bib linkers to give rise to a complicated 3D network with the small solvent-accessible void space (equal to 1.5% of the cell volume) (Figure 2b).[16] In the packing arrangement of **1**, these [-Co-bib-Co-bib-Co-]$_n$ left-and right-handed helical chains are present in equal numbers but run perpendicular to each other (giving a full racemic compound) (Figure 2c). Better insight into the elegant framework of **1** can be accessed by the topology method. In this analysis, the metal center can be viewed as 4-connect node. In this way, this net can be simplified as $CdSO_4$ topology.[17] Moreover, the occurrence of 3-fold interpenetration and polycatenane character are also observed, as shown in Figure 2d−f.

In the open framework, the quadrangular channel is made up of one-dimensional (1D) 2_1 left- or right-handed helical chains. The two helical chains result from metal−ligand interaction with the same composition of (-Co-L1-Co-bib-Co-)$_n$. The most striking feature of **1** is the mixed interweaving of the helical chains due to the interpenetration fashion. Upon the 3-fold interpenetration, the resulting identical helices from related interpenetrated layers intertwine together

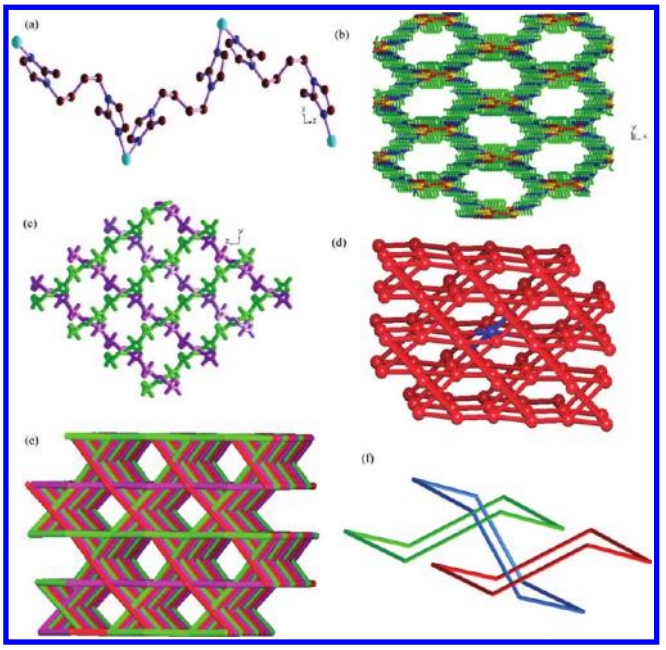

Figure 2. (a) A zigzag chain directed by metal centers and bib ligands; (b) the 3D micropous metal−organic framework; (c) the stacking mode for 1D zigzag chain directed by metal centers and bib ligands; (d) schematic diagram of $CdSO_4$ topology; (e) view of 3-fold interpenetrating net; (f) schematic diagram of polycatenane motif in **1**.

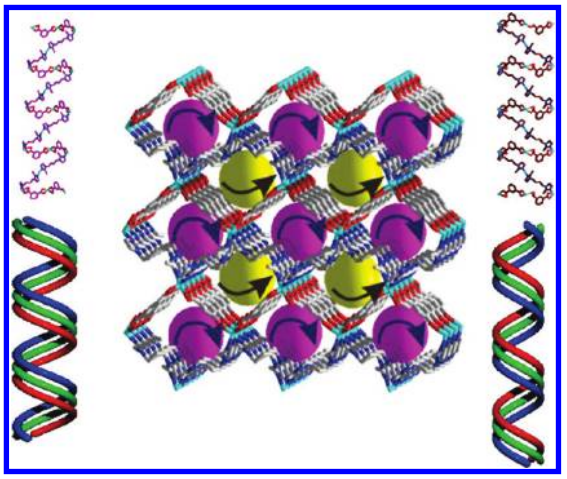

Figure 3. View of left-and right-handed helical chains.

to generate three-stranded left-or right-handed helices, as described in Figure 3. To the best of our knowledge, compound **1** is the first example that has the interweaving of triple-stranded helices, which are constructed by replacing bis(imidazole) and carboxylate ligands.

{[Co(L2)(bib)]·1.5H$_2$O}$_n$ (2). A flexible aliphatic dicarboxylate ligand L2 was used instead of L1. A new 3D complicated architecture was formed in **2** under similar reaction conditions. As illustrated in Figure 1b, the asymmetry unit consists of one independent Co(II) atom, one L2, one bib ligand, and one and a half lattice water molecules. The Co(II) is ligated by two oxygen atoms from two adjacent L1 ligands and two nitrogen atoms from bib linkers to give the CoO2N2 tetrahedral geometry. The Co−O/N bond lengths are comparable to those in **1**. The bib adopts a *syn-anti* configuration with the planes of the two imidazole rings inclined by 31.11°, and the Co···Co separation across the

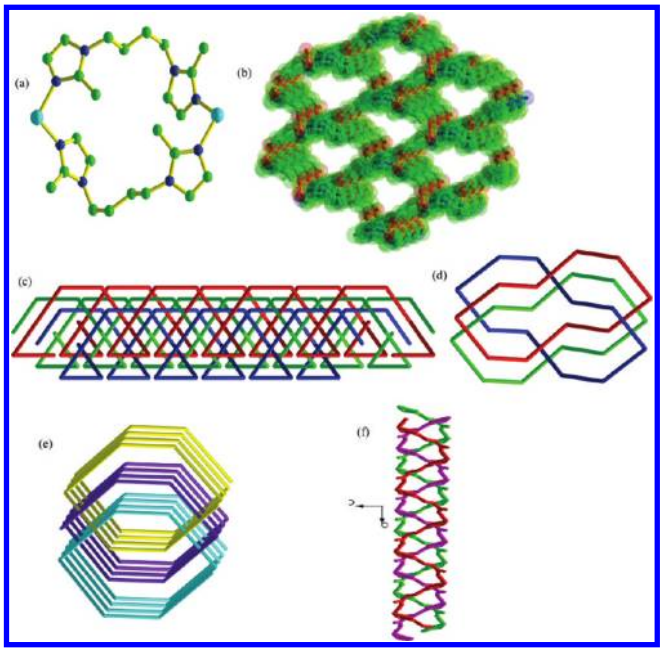

Figure 4. (a) The molecular ring formed by bib and metal atoms; (b) the 3D micropous metal−organic framework; (c) framework perspective of **2** showing the 3-fold interpenetrating motif with **ThSi$_2$**-type network; (d) view of pseudo-Borromean; (e) a view down *c* of the three 1D tubular channels; (f) view down *b* axis of triply stranded helix.

bib ligand is 10.2 Å. Two bib molecules link two Co(II) atoms to generate a loop (Figure 4a). Each L2 anion adopts a bi(monodentate) coordinative mode. The extension of the structure into a 3D network is accomplished by flexible L2 anions (Figure 4b).

Along the *b* axis, in the porous complex there is one type of rhombic channel, which is occupied by water molecules. The total solvent volume in the lattice is about 455 Å^3 (5.7% of the unit cell) using the *PLATON* suite of program. A 3-connected **ThSi$_2$** network is generated if the nodes are defined as being the loop. This is different from the usual diamond topology for a 3-connected network, and only a few structures with two flexible coligands have been reported. The large voids formed by a single 3D net allow incorporation of other two identical nets, thus giving a 3-fold interpenetrating motif with *pseudo*-Borromean links, as described in Figure 4c,d. Upon the 3-fold interpenetration, three identical helical tubes from related interpenetrated layers intertwine the central one along the *a* axis with the extent of intercalation of about 0.56 nm (Figure 4e). The other three helical chains [-Co-L2-Co]$_n$ are directed in the same direction, as shown in Figure 4f.

{[Co(L3)(bib)$_{0.5}$]·0.5H$_2$O}$_n$ (3). When a new type of aromatic dicarboxylate L3 ligand was introduced in the Co-bib system, compound **3** with a pillared structure was isolated. It displays a new 3D network based on the paddle-wheel building block. Figure 1c illustrates the coordination environment of the Co(II) atom and 6-fold connectivity of the bimetallic unit. Each Co(II) atom in the binuclear unit is coordinated by four carboxylic oxygen atoms of L3 ligands and one nitrogen atom of bib ligand adopting the *syn-anti* coordinated fashion to furnish a square-pyramidal geometry. Two crystallopraphically equivalent Co(II) atoms are connected by four carboxylate ends binding in bridging bis(bidentate) mode to give a paddle-wheel shaped [Co$_2$(RCO$_4$)$_4$] fragment,

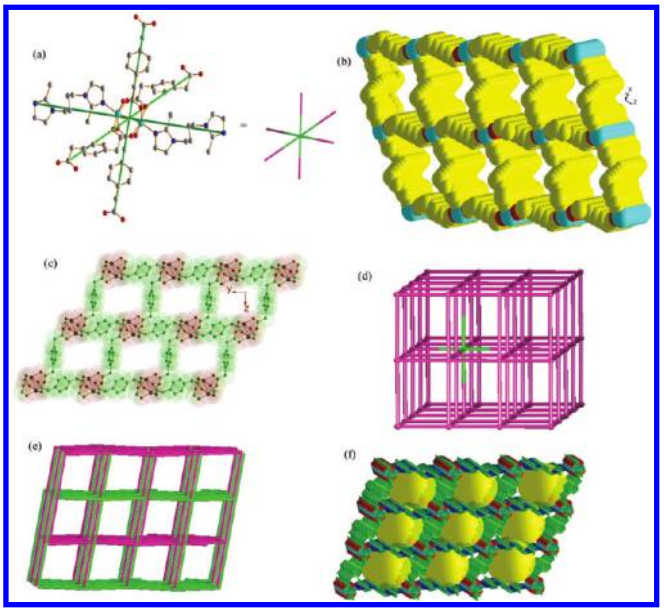

Figure 5. (a) Schematic diagram of six-connected node for binuclear unit of **3**; (b) the 3D micropous metal−organic framework; (c) the 2D sheet shaped by L3 and metal centers; (d) schematic representation of **Pcu**-type topology; (e) viewing of the 2-fold interpenetrated network; (f) view of the rhombic channels.

in which the Co···Co separation across is 2.87(2) Å. The axis sites of each paddle-wheel unit are occupied by two additional bib linkers via nitrogen atoms. Therefore, an arrangement where the carboxylate carbons atoms and imidazole nitrogen atoms are connected in turn constitutes an octahedral [Co$_2$(RCO$_4$)$_4$N$_2$] building block. Each octahedral [Co$_2$(RCO$_4$)$_4$N$_2$] building block acting as a node (Figure 5a) is connected by six identical sets through four bridging L3 and two bib ligands to afford an extended 3D motif (Figure 5b), which can also be considered as being constructed by distorted 2D square-grid (4,4) layers of composition [Co(L3)] pillared by bib ligands (Figure 5c). From the topological view, the whole 3D motif can be classified as a classical **Pcu** architecture.[18] The large voids directed by a single 3D net allow incorporation of one identical motif, providing a 2-fold interpenetrating network, as shown in Figure 5d. Some similar topological frameworks have been constructed by flexible carboxylate and bis(imidazole) coligands. We have noticed that most examples of **Pcu** topology are constructed by a paddle-wheel unit, which is formed by four μ_2-bridging carboxylate linkers and linear N-donor ligands.[19]

In addition, along the *a* axis, in the porous complex there is one type of rhombic channel, which is occupied by water molecules (Figure 5e). The total solvent volume in the lattice is about 78.5 Å^3 (9.1% of the unit cell) by calculation using the *PLATON* suite of program.

Comparison of the Structures of Coordination Polymers

The simultaneous use of the flexible and rigid dicarboxylate ligands in the presence of flexible bis(imidazole) ligand affords diverse entangled networks, as shown in Scheme 2. Although we are unable to propose definitive reasons as to why the compounds exhibit different topologies with our present state of knowledge, some of the general trends observed are discussed below.

Effect of Carboxylate Anions. As we know, in the generation of ternary MOFs, carboxylate linkers play an important

Scheme 2. Schematic Representations of the Three Types of Interpenetrated Motifs Modulated by Different Conformations of Dicarboxylate Ends

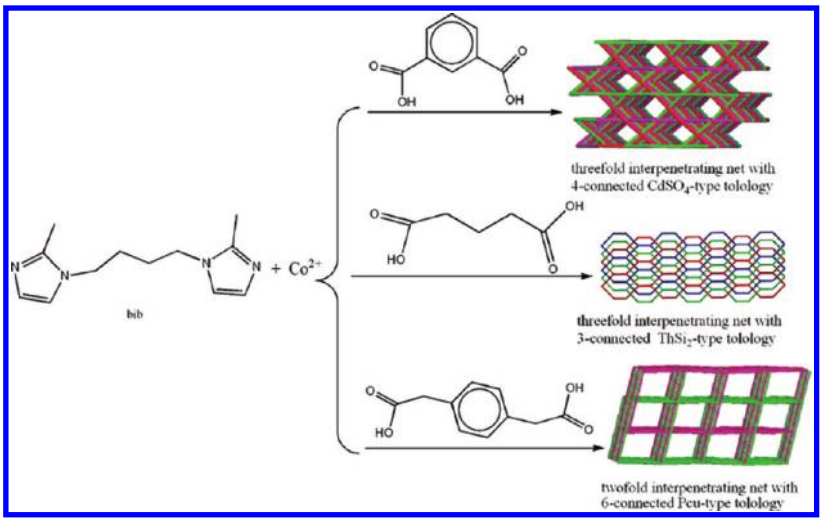

role in the formation resulting structures. So we herein have employed three types of dicarboxylate ligands viewing their distinct configuration and rigidity. As described above, when the aromatic rigid L1 was introduced into the Co-bib system, a 3D 4-connected 3-fold interpenetrating $CdSO_4$ motif in **1** was formed. In a $[Ni(L)(NDC)]_n$ (L = 1,1′-(1,4-butanediyl)-bis(imidozole) and NDC = 1,2-benzenedicarboxylate) polymer, although it displays similar 3D 4-connected $CdSO_4$ topology,[10a] the characters of interpenetration and the helical tube are not observed. L2 is an aliphatic dicarboxylate ligand and possesses flexibility owing to the presence of a $-CH_2-CH_2-CH_2-$ spacer between the two carboxylate moieties, which could conform to the requirements of the coordination geometries of metal ions in the assembly process. An intriguing 3D 3-fold interpenetrating **$ThSi_2$** architecture was obtained. Yang and his co-workers reported a $[Cu(suc)(L)]_n \cdot 3nH_2O$ (H_2suc = succinic acid and L = 1,1′-(1,4-butanediyl)bis(imidozole)) complex; it reveals an unusual Archimedean-type net containing two different types of nodes.[10b] Though the coordination geometries of the metal centers are identical, two different connected nodes and topologies were obtained in **1** and **2**. The difference between the two framework topologies, with coordinated parameters of carboxylates remaining the same, can be attributed to the conformations of assistant ligands. In contrast, when an aromatic flexible 1,4-phenylenediacetic acid is introduced, a binuclear unit is formed in polymer **3**. It has 3D 2-fold interpenetrating **Pcu** topology. In a $[Zn(bdc)(L)_{0.5}]$ (bdc = 1,4-benzenedicarboxylate) compound,[19] it possesses a Zn-paddle-wheel unit and exhibits 3-fold interpenetrating **Pcu**-type topology. Therefore, the conformations of carboxylate ligands influence the metal nuclearity and hence the connectivity of resulting motif. Upon further comparison of **1** and **3**, we noticed the paddle-wheel unit of metal centers was formed in **3**, and moreover, the coordination mode of carboxylate ligand was changed. Consequently, the connected nodes and interpenetrating dimensions are also different. Such result also implies that the different conformations of carboxylates have a critical role in the resulting frameworks.

Thermogravimetric Analyses

The decomposition behaviors of **1**−**3** were examined via TGA (Figure S1, Supporting Information). Compound **1** shows one weight loss step. For **2**, the weight loss in the range 30−195 °C corresponds to the departure of H_2O (obsd 4.8%, calcd 5.4%). Compound **3** also has two observed weight losses; first weight loss of 3.1% corresponds to the loss of the crystallization water molecules (calcd 2.2%).

Additionally, to confirm the phase purity and stability of compounds **1**−**3**, the original sample was both characterized by X-ray powder diffraction (XRPD) at room temperature. The patterns that were simulated from the single-crystal X-ray data of compounds were in agreement with those that were observed (Figure S2, Supporting Information). XRPD patterns of compounds **1** and **3** were recorded at 350 and 300 °C, respectively, which indicates that are able to survive.

Magnetic Property

The variable-temperature magnetic susceptibility was measured from 1.8 to 300 K at 1000 Oe for **3**. The magnetic data of **3** are displayed in Figure S3, Supporting Information, plotted as the thermal variation of $\chi_M T$, χ_M, and $1/\chi_M$. The $\chi_M T$ vs T plot has a value of 2.29 $cm^3\ mol^{-1}$ K, which is a little larger than the spin-only value (1.875 $cm^3\ mol^{-1}$ K) for $S = 3/2$ per formula unit.[20] ${\chi_M}^{-1}$ obeys the Curie−Weiss law with a Curie constant of 4.62 cm^3 K mol^{-1} and a Weiss constant of $\theta = -3.39$ K. The negative θ value is indicative of a dominant antiferromagnetic interaction between Co^{2+} centers. According to the structure of compound **3**, it could be presumed that the main magnetic interactions are between the paddle-wheel unit metal center, while the superexchange interactions between Co ions through the bib bridge can be ignored due to the length of the bib ligands, as shown in Figure S4, Supporting Information.[21]

Conclusion

In summary, three new Co(II) coordination polymers with different interpenetrating and topological motifs have been isolated through varying the assistant dicarboxylates. These results herein indicate that the conformations of carboxylates have a great influence on the structures of resulting metal−organic frameworks and also reveal that the introduction of methyl groups into the imidazole skeleton is an efficient method for construction of new MOFs. It is believed that more MOFs containing flexible bis(imidazole) and polycarboxylate anions with interesting structures as well as physical properties will be documented.

Acknowledgment. This work was partially supported by the grants from Guangdong Medical College and National Nature Science Foundation of China (No. 81001622).

Supporting Information Available: Figure S1: TG curves of the complexes. Figure S2: Comparison of XRPD patterns of the simulated pattern from the single-crystal structure determination, the as-synthesized products in compounds **1**−**3** (a−c). Figure S3: Plots of $\chi_M T$, χ_M, and χ_M^{-1} versus T for **3**. Figure S4: Schematic representation of magnetic interaction in paddle-wheel unit for compound **3**. Table S1: Kinds of features of MOFs with bim ligand. This material is available free of charge via the Internet at http://pubs.acs.org.

References

(1) (a) Long, J. R.; Yaghi, O. M. *Chem. Soc. Rev.* **2009**, *38*, 1213. (b) Murray, L. J.; Dinca, M.; Long, J. R. *Chem. Soc. Rev.* **2009**, *38*, 1294. (c) Yaghi, O. M.; O'Keeffe, M.; Ockwig, N. W.; Chae, H. K.; Eddaoudi, M.; Kim, J. *Nature* **2003**, *423*, 705. (d) Leininger, S.; Olenyuk, B.; Stang, P. J. *Chem. Rev.* **2000**, *100*, 853. (e) Bradshaw, D.; Claridge, J. B.; Cussen, E. J.; J. Prior, T.; Rosseinsky, M. J. *Acc. Chem. Res.* **2005**, *38*, 273. (f) Ma, S. Q.; Eckert, J.; Forster, P. M.; Yoon, J.; Hwang, Y. K.; Chang, J. S.; Collier, C. D.; Parise, J. B.; Zhou, H. C. *J. Am. Chem. Soc.* **2008**, *130*, 15896. (g) Ma, L. F.; Wang, L. Y.; Du, M.; Batten, S. R. *Inorg. Chem.* **2010**, *49*, 365. (h) Ma, L. F.; Liu, B.; Wang, L. Y.; Li, C. P.; Du, M. *Dalton Trans* **2010**, *39*, 2301. (i) Ma, L. F.; Meng, Q. L.; Li, C. P.; Li, B.; Wang, L. Y.; Du, M.; Liang, F. P. *Cryst. Growth Des.* **2010**, *10*, 3036.

(2) (a) Lee, S. J.; Lin, W. *J. Am. Chem. Soc.* **2002**, *124*, 4554. (b) Wang, J.-G.; Huang, C.-C.; Huang, X.-H.; Liu, D.-S. *Cryst. Growth Des.* **2008**, *8*, 795. (c) Sun, Y.-Q.; Zhang, J.; Chen, Y.-M.; Yang, G.-Y. *Angew.Chem., Int. Ed.* **2005**, *44*, 5814. (d) Zhou, Y. F.; Hong, M. C.; Wu, X. T. *Chem.Commun.* **2006**, 135. (e) Wang, F.-Q.; Zheng, X.-J.; Wan, Y.-H.; Sun, C.-Y.; Wang, Z.-M.; Wang, K.-Z.; Jin, L.-P. *Inorg. Chem.* **2007**, *46*, 2956. (f) Chen, C.-L.; Kang, B.-S.; Su, C.-Y. *Aust. J. Chem.* **2006**, *59*, 3. (g) McKinlay, A. C.; Morris, R. E.; Horcajada, P.; Férey, G.; Gref, R.; Couvreur, P.; Serre, C. *Angew.Chem., Int. Ed.* **2010**, *49*, 6260.

(3) (a) Férey, G.; Serre, C. *Chem. Soc. Rev.* **2009**, *38*, 1380. (b) Robson, R. *Dalton Trans* **2008**, 5113. (c) Perry, J. J., IV; Perman, J. A.; Zaworotko, M. J. *Chem. Soc. Rev.* **2009**, *38*, 1400. (d) Du, M.; Zhang, Z. H.; Tang, L. F.; Zhao, X. J.; Batten, S. R. *Chem.*−*Eur. J.* **2007**, *13*, 2578. (e) Wang, X. L.; Qin, C.; Wang, E. B.; Li, Y. G.; Su, Z. M.; Xu, L.; Carlucci, L. *Angew. Chem., Int. Ed.* **2005**, *44*, 5824. (f) Hou, L.; Lin, Y. Y.; Chen, X. M. *Inorg. Chem.* **2008**, *47*, 1346. (g) Xue, D. X.; Lin, J. B.; Zhang, J. P.; Chen, X. M. *CrystEngComm* **2009**, *11*, 183.

(4) (a) Carlucci, L.; Ciani, G.; Gramaccioli, A.; Proserpio, D. M.; Rizzato, S. *CrystEngComm* **2000**, *29*, 1. (b) Batten, S. R.; Robson, R. *Angew. Chem., Int. Ed.* **1998**, *37*, 1461. (c) Carlucci, L.; Ciani, G.; Proserpio, D. M. *Coord. Chem. Rev.* **2003**, *246*, 247. (d) Long, D. L.; Hill, R. J.; Blake, A. J.; Champness, N. R.; Hubberstey, P.; Wilson, C.; Schröder, M. *Chem.*—*Eur. J.* **2005**, *11*, 1384.

(5) (a) Ha, S. M.; Yuan, W.; Pei, Q.; Pelrine, R.; Stanford, S. *Adv. Mater.* **2006**, *18*, 887. (b) Liu, C. M.; Gao, S.; Zhang, D. Q.; Huang, Y. H.; Xiong, R. G. *Angew. Chem., Int. Ed.* **2005**, *117*, 72. (c) Wang, H. Y.; Gao, S.; Huo, L. H.; Ng, S. W.; Zhao, J. G. *Cryst. Growth Des.* **2008**, *8*, 665. (d) Ockwig, N. W.; Delgado-Friederichs, O.; O'Keeffe, M.; Yaghi, O. M. *Acc. Chem. Res.* **2005**, *38*, 176. (e) Mulfort, K. L.; Farha, O. K.; Malliakas, C. D.; Kanatzidis, M. G.; Hupp, J. T. *Chem.*−*Eur. J.* **2009**, *10*, 889.

(6) (a) Li, J.; Furuta, T.; Goto, H.; Fujiwara, Y.; Yip, S. J. *Chem. Phys.* **2003**, *119*, 2376. (b) Kesanli, B.; Cui, Y.; Smith, R. M.; Bittner, E. W.; Bockrath, C. B.; Lin, W. B. *Angew. Chem., Int. Ed.* **2005**, *117*, 72.

(7) (a) Guo, H. D.; Qiu, D. F.; Guo, X. M.; Zheng, G. L.; Wang, X.; Dang, S.; Zhang, H. J. *CrystEngComm* **2009**, *11*, 2425. (b) Luo, F.; Yang, Y. T.; Che, Y. X.; Zheng, J. M. *CrystEngComm* **2008**, *10*, 981. (c) Zhang, L. P.; Yang, J.; Ma, J. F.; Jia, Z. F.; Xie, Y. P.; Wei, G. H. *CrystEngComm* **2008**, *10*, 1410. (d) Duan, X. Y.; Cheng, X.; Lin, J. G.; Zang, S. Q.; Li, Y. Z.; Zhu, C. J.; Meng, Q. J. *CrystEngComm* **2008**, *10*, 706.

(8) (a) Cui, G. H.; Li, J. R.; Tian, J. L.; Bu, X. H.; Batten, S. R. *Cryst. Growth Des.* **2005**, *5*, 1775. (b) Lan, Y. Q.; Li, S, L.; Su, Z. M.; Shao, K. Z.; Ma, J. F.; Wang, X. L.; Wang, E. B. *Chem. Commun.* **2008**, 58. (c) Kim, H.; Suh, M.Y. P.I *norg. Chem* **2005**, *44*, 810. (d) Mondal, R.; Bhunia, M. K.; Dhara, K. *CrystEngComm* **2008**, *10*, 1167.

(9) (a) Zhang, X. M.; Hao, Z. M.; Zhang, W. X.; Chen, X. M. *Angew. Chem., Int. Ed.* **2007**, *46*, 3456. (b) Hu, S.; Zhou, A. J.; Zhang, Y. H.; Ding, S.; Tong, M. L. *Cryst. Growth Des.* **2006**, *6*, 2543. (c) Wang, D. X.; He, H. Y.; Chen, X. H.; Feng, S. Y.; Niu, Y. Z.; Sun, D. F. *CrystEngComm* **2010**, *2*, 1041. (d) Wang, H. L.; Zhang, D. P.; Sun, D. F.; Chen, Y. T.; Wang, K.; Ni, Z. H.; Tian, L. J.; Jiang, J. Z. *CrystEngComm* **2010**, *12*, 1096. (e) Guo, H. D.; Qi, D. F.; Guo, X. M.; Batten, S. R.; Zhang, H. J. *CrystEngComm* **2009**, *11*, 2611. (f) Zhang, Z. H.; Du, M. *CrystEngComm* **2008**, *10*, 1350.

(10) (a) Qi, Y.; Luo, F.; Che, Y. X.; Zheng, J. M. *Cryst. Growth Des.* **2008**, *8*, 606. (b) Yang, J.; Ma, J. F.; Liu, Y. Y.; Li, S. L.; Zheng, G. L. *Eur. J. Inorg. Chem.* **2005**, 2174. (c) Dong, B. X.; Peng, J.; Gómez-Gara, C. J.; Benmansour, S.; Jia, H. Q.; Hu, N. H. *Inorg. Chem.* **2007**, *46*, 5933. (d) Li, X. J.; Cao, R.; Bi, W. H.; Wang, Y. Q.; Wang, Y. L.; Li, X.; Guo, Z. G. *Cryst. Growth Des.* **2005**, *5*, 1651. (e) Li, S. L.; Lan, Y. Q.; Ma, J. F.; Yang, J.; Wei, G. H.; Zhang, L. P.; Su, Z. M. *Cryst. Growth Des.* **2008**, *8*, 675. (f) Zhang, W. L.; Liu, Y. Y.; Ma, J. F.; Jiang, H.; Yang, J.; Ping, G. J. *Cryst. Growth Des.* **2008**, *8*, 1250. (g) Wen, L. L.; Lu, Z. D.; Lin, J. G.; Tian, Z. F.; Zhu, H. Z.; Meng, Q. J. *Cryst. Growth Des.* **2007**, *7*, 93. (h) Qi, Y.; Luo, F.; Batten, S. R.; Che, Y. X.; Zheng, J. M. *Cryst. Growth Des.* **2008**, *8*, 2806. (i) Meng, X. G.; Song, Y. L.; Hou, H. W.; Han, H. Y.; Xiao, B.; Fan, Y. T.; Zhu, Y. *Inorg. Chem.* **2004**, *43*, 3528.

(11) Carlucci, L.; Ciani, G.; Proserpio, D. M.; Rizzato, S. *Chem.*—*Eur. J.* **2002**, *8*, 1519.

(12) Huang, X. Y.; Yue, K. F.; Jin, J. C.; Liu, J. Q.; Wang, C. J.; Wang, Y. Y. *Inorg. Chem. Commun.* **2010**, *3*, 338.

(13) Sheldrick, G. M. *SHELXL-97: Program for Structure Determination and Refinement*; University of Göttingen: Göttingen, 1997.

(14) Sheldrick, G. M. *SADABS 2.05*; University of Göttingen: Germany, 2002.

(15) Luo, F.; Che, Y. X.; Zheng, J. M. *Eur. J. Inorg. Chem.* **2007**, 3906.

(16) Spek, A. L. *PLATON, A Multipurpose Crystallographic Tool*; Utrecht University: Utrecht, The Netherlands, 2001.

(17) (a) Batten, S. R.; Robson, R. In *Molecular Catenanes, Rotaxanes and Knots: A Journey Through the World of Molecular Topology*; Sauvage, J.-P., Dietrich-Buchecker, C., Eds.; Wiley-VCH: Weinheim, 1999; pp 77. (b) Ockwig, N. W.; Delgado-Friederichs, O.; O'Keeffe, M.; Yaghi, O. M. *Acc. Chem. Res.* **2005**, *38*, 176. (c) Wells, A. F. *Three-Dimensional Nets and Polyhedra*; Wiley-Interscience: New York, 1977.

(18) Wang, X. L.; Qin, C.; Wang, E. B.; Shu, Z. M. *Chem.*—*Eur. J.* **2006**, *12*, 2680.

(19) Abrahams, B. F.; Hoskins., B. F.; Robson, R. *CrystEngComm* **2002**, *4*, 748.

(20) (a) Duan, Z. M.; Zhang, Y.; Zhang, B.; Zhu, D. B. *Inorg. Chem.* **2008**, *47*, 9152. (b) Zhang, W. H.; Wang, Y. Y.; Lermontova, E. K. L.; Yang, G. P.; Liu, B.; Jin, J. C.; Dong, Z.; Shi, Q. Z. *Cryst. Growth Des.* **2010**, *10*, 76. (c) Shi, Q.; Sun, Y. T.; Sheng, L. Z.; Ma, K. F.; Cai, X. Q.; Liu, D. S. *Inorg. Chimi. Acta.* **2009**, *362*, 4167.

(21) Li, Y. G.; Hao, N.; Wang, E. B.; Lu, Y.; Hu, C. W.; Xu, L. *Eur. J. Inorg. Chem.* **2003**, 2567.